Diffusion and Rheology of Binary Polymer Mixtures

Shanfeng Wang, Ernst D. von Meerwall, Shi-Qing Wang,* A. Halasa,† W.-L. Hsu,† J. P. Zhou,† and R. P. Quirk

Maurice Morton Institute of Polymer Science and Department of Polymer Science, The University of Akron, Akron, Ohio 44325

Received June 19, 2003; Revised Manuscript Received October 31, 2003

ABSTRACT: This work studies the diffusion and rheological behavior of binary mixtures (of long and short chains) based on 1,4-polybutadiene over the full composition range as a function of both long and short chain lengths using pulse-gradient NMR spin echo and oscillatory shear measurements. The first set of rheological and diffusion measurements reveals that the terminal relaxation rate $1/\tau_d$ and self-diffusion coefficient D_s of the long chains both decrease systematically with increasing short chain length N_S and with the weight fraction ϕ of the long chain in the mixtures. The second set of data indicates that the short chain's diffusion coefficient D_s decreases with increasing ϕ, leading to insightful comparison between the self-diffusion coefficient D_s at $\phi = 0$ and trace diffusion coefficient D_{tr} in the limit of $\phi = 1.0$: D_{tr} recovers the asymptotic molecular weight scaling of $M^{-2.0}$, whereas D_s scales nonideally as $M^{-2.4}$ due to the considerable constraint release effect in the explored range of molecular weight. Third, short chains of molecular weight below M_e are found to diffuse in entangled matrices of different chain length N_L with a self-diffusion coefficient D_s that is independent of N_L at all compositions.

I. Introduction

Polymer diffusion is a ubiquitous phenomenon that dictates a great number of dynamic processes including adhesion, phase separation through spinodal decomposition, and mixing. The subject is also intimately related to the topic of molecular rheology of polymers. Over the past three decades or so, the matter of chain diffusion and relaxation dynamics has been extensively studied from all perspectives ranging from molecular modeling,[1−3] measurements of self-and tracer/trace diffusion using a wide range of experimental techniques[4−7] (e.g., pulsed-gradient NMR, forward recoil spectrometry (FRES), forced Rayleigh scattering, infrared spectroscopy) to oscillatory shear measurements[8−11] to determine the terminal relaxation behavior. Apart from polymer solutions for which a great deal of work has been carried out,[12−16] much of the past research focused on monodisperse samples in order to gain a basic understanding of chain dynamics in this ideal limit of uniform chain length.[4,16−23]

Despite a great deal of efforts,[24,25] some major controversies remain even for the simplest case of monodisperse entangled polymers. Extensive data in the literature indicate the molecular weight scaling of the relaxation time τ_d or zero-shear viscosity η_0 as M^μ with $\mu = 3.4$ and that of the tracer diffusion coefficient D_{tr} as $M^{-2.0}$. On the other hand, self-diffusion measurements tend to show D_s as $M^{-\nu}$ with $\nu > 2.0$. The deviation of the exponent 3.4 from 3.0 is generally believed to arise from the contour length fluctuation (CLF).[2,26,27] The origin of the exponent $\nu > 2.0$ has been a subject of debate. After a thorough survey of all available experimental observations, a suggestion has been emphasized in a recent review article[28] that CLF has little effect on chain diffusion, i.e., chain diffusion and stress relaxation do not share the same physics, and that the observed nonasymptotic scaling of the self-diffusion coefficient $D_s \propto M^{-\nu}$ with $\nu > 2.0$ stems from the constraint release (CR) effect,[29] which can be removed by immersing the probe/trace chains in a matrix of significantly higher molecular weight (which leads to the trace diffusion results). On the other hand, there have also been both experimental and theoretical indications to suggest the origin of the difference between 3.4 and 3.0 to also come from the CR effect.[30−33] In other words, CLF would have no effect on the disentanglement time τ_d, and thus the ideal reptative scaling of $M^{3.0}$ would appear upon embedding the relaxing chains in a matrix of sufficiently higher molecular weight to remove the CR correction. This interpretation would also provide an explanation for the observed scaling for $D_{tr} \propto M^{-2.0}$. New experiments must be carried out to determine whether CR would play a more dominant role than CLF to affect the chain relaxation dynamics.

There has been a significant amount of work on rheology of entangled binary mixtures from the viewpoints of both theory and experiment.[8−11,34−40] In the case where the relaxation time of the long chain is significantly longer than that of the short chain, it is straightforward to measure, using oscillatory shear, the disentanglement dynamics associated with the long chain and to determine the influence of short chains of different length N_S at various weight fractions of the long chain. Moreover, the terminal relaxation dynamics of such binary mixtures can actually be rationalized within a tube model for chain reptation that incorporates the notions of tube dilation and coarse-grained curvilinear diffusivity of the reptating chain.[11] This model appears to have extended the range of application of previous theories.[34,35] The present work offers new experimental results from diffusion measurements to further test the proposed theoretical framework. On the other hand, the disentanglement dynamics associated with the short chain in its binary mixtures with long chains are difficult to identify with conventional rheological characterization techniques.

† Chemical Division Research and Development, Goodyear Tire and Rubber Company, Akron, OH 44305.

* Corresponding author: e-mail swang@uakron.edu.

10.1021/ma034835g CCC: $27.50
Published on Web 01/20/2004

Table 1. Molecular Characteristics of PBD Samples

sample	% 1,4	% 1,2	M_n	M_w	M_w/M_n	T_g (°C)
44K	91.7	8.3	43500	43900	1.01	−100.0
12K	91.4	8.6	11300	11600	1.03	−100.9
8.9K	91.4	8.6	8500	8900	1.04	−102.5
5.8K	91.0	9.0	5500	5800	1.06	−102.0
3.9K	90.1	9.9	3500	3900	1.10	−101.9
2.0K			1500	2000	1.33	−103.0
1.0K	90.0	10.0	900	1000	1.15	−105.4
0.7K			700	800	1.08	−106.8

We can, nevertheless, make self-diffusion measurements of *both* long and short chains in binary mixtures. Rheological characteristics associated with the long chains in these mixtures can also be made using the standard rheological method (i.e., oscillatory shear). Such parallel studies of both diffusion and rheology of mixtures potentially offer a rare opportunity to compare these properties, at least for the long chains, and to determine whether chain diffusion and relaxation processes are equivalent. Simultaneous measurements of both diffusion and rheological properties have previously been performed only for pure melts and solutions[16,18,21] and are actually quite rare in the literature. More evidently, the present study represents the first systematic diffusion measurements of long and short chains in strongly entangled binary mixtures in the full concentration range although there exist some scattered data on diffusion coefficient of the long chain in short chains at finite concentrations by PG-NMR,[41−44] fluorescence redistribution after pattern photobleaching (FRAPP),[45] and FRES.[46,47] Most of these previous diffusion studies involved either unentangled or marginally entangled short chains in binary mixtures so that the systems were more like entangled solutions than binary mixtures where both components are themselves well entangled.

In this work we have characterized diffusion and rheological behavior of 1,4-polybutadiene (PBD) binary mixtures at different weight fractions of the long chains for various short chain lengths, where the molecular weights of monodisperse PBD range from 0.7K to 44K. When the long and short chain lengths are sufficiently different to separate the time scales associated with their dynamics, the rheological measurements allow evaluation of the terminal relaxation dynamics associated with the long chains. On the other hand, the pulsed-gradient NMR (PG-NMR) method makes simultaneous determination possible of the self-diffusion coefficients associated with both long and short chains in the binary mixtures at various compositions. These measurements reveal that (a) the long chain dynamics depend not only on its weight fraction in the binary mixture but systematically vary with the short chain length and (b) constraint release speeds up chain diffusion and causes it to have nonreptative molecular weight dependence. Some of these experimental data have been reported recently.[48]

II. Experimental Section

Synthesis and Characterization. Our model mixtures consist of linear 1,4-polybutadiene (PBD) all synthesized and analyzed in the Goodyear Research Center except for the last two samples in Table 1, which were made at the University of Akron. All the PBD samples were prepared under vacuum line condition by anionic polymerization. A column (packed with silica, molecular sieve, and alumina) dried premix containing 20 wt % of 1,3-butadiene in hexanes was charged into a stirred 1 gallon glass reactor at room temperature. The monomer concentration was determined by gas chromatography (GC). After the impurity level of the premix was determined, the premix was heated to 65 °C, and a desired amount of initiator (*n*-butyllithium in hexane) was added to initiate the polymerization. The progress of the polymerization was monitored by analyzing the residual monomer left in the polymerization mixture by GC. After the polymerization was completed (usually less than 2 h at 65 °C), a small amount of ethanol was added to shortstop the polymer live ends. One weight percent antioxidant (BHT) was added to the polymer cement. The cement was then coagulated with ethanol. The resulting polybutadiene product was dried at 50 °C under vacuum. The preparation for the lowest two molecular weight samples was different. The calculated volume of purified butadiene was condensed into the ampule using a dry ice/isopropyl alcohol bath (−78 °C). After the solvent was completely thawed, butadiene monomer was poured immediately into the reactor containing *sec*-butyllithium initiator and cyclohexane by breaking the corresponding break-seal. The polymerization was carried in a temperature controlled ice water bath for 24 h. The living polymer was terminated by addition of deoxygenated methanol. The polymer was precipitated into methanol with preadded 0.5 wt % BHT (of polymer). The polymer was isolated by decantation and dried in a vacuum oven over 2 days as a clear liquid.

The molecular weight and the polydispersity were determinated by gel permeation chromatography. The vinyl content was determined by ^{1}H NMR. Table 1 shows the molecular characteristics of these samples, 2.0K and 0.7K are also 1,4-PBD although the detailed microstructures were not determined at the present. The binary mixtures were prepared at the long chain's weight fractions equal to 80%, 50%, 20%, and 10%. Some binary mixtures had other concentrations such as 60%, 40%, and 5%. Weighed amounts of long and short chain melts were dissolved in toluene over 2−3 days in the dark at room temperature, with periodic manual stirring. After achieving a uniform solution, toluene was then removed under vacuum at room temperature for at least 1 week until the samples contained less than 0.2% of toluene.

Rheological Measurements. Linear viscoelastic properties of the PBD mixtures were measured by a dynamic mechanical spectrometer (Advanced Rheometrics Expansion System-ARES) at frequencies ranging from 0.1 to 100 rad/s and various temperatures between −80 and 40 °C. Measurements on low molecular weight samples were carried out at temperature not lower than −40 °C to avoid crystallization.[49] For the highest molecular weight sample (M = 44K) and its blends containing unentangled short chains, for example, PBD44K in 1.0K, the crystallization produced a negligible effect on the rheological properties even at temperatures as low as −80 °C. The spectrometer is equipped with a 200−2000 g cm dual range, force rebalance transducer, and oscillatory shear measurements were carried out using a 25 mm diameter parallel plate flow cell. Gap settings of 0.5−1 mm were used. A small strain ($\gamma_0 < 0.05$) was always used when $|G^*|$ was large, and no strain amplitudes were larger than 0.20.

Oscillatory shear experiments were carried out to measure the storage and loss moduli G' and G'' of binary mixtures made of monodisperse high molecular weight and low molecular weight 1,4-polybutadienes. At high concentrations ($\phi > 0.50$), the data obtained at different temperatures were reduced to master curves at the reference temperature of 40 °C. Several important rheological properties can be evaluated from the master curves for G' and G'', including the zero-shear viscosity and terminal relaxation time or disentanglement relaxation time. To make a comparison with the diffusion data obtained at the temperature of 110.5 °C, both steady shear viscosity at low shear rates and dynamic viscosity at low frequencies were also measured at 110.5 °C. All values of the zero-shear viscosity for both pure melts and binary mixtures at reference temperatures are given in Table 2. All data in Table 2 carry an experimental error of at least 5%.

Pulsed-Gradient Diffusion Measurements. The specimens used in the NMR diffusion measurements, both pure

Table 2. Viscosities of PBD Mixtures at 40 and 110.5 °C[a]

	η (Pa s) at ϕ =									
mixture	1.0	0.8	0.6	0.5	0.4	0.2	0.1	0.05	0.02	0
44K/12K	1500 (200)	840	420	270	167	54	26			13 (1.7)
44K/8.9K	1500 (200)	770		250		35	14	8.7		5.4 (0.79)
44K/5.8K	1500 (200)	780		190		19	6.1			1.7 (0.27)
44K/3.9K	1500 (200)	750	290	190		18	4.9			0.70 (0.13)
44K/2.0K	1500 (200)	690		160		12	3.8			0.22 (0.04)
44K/1.0K	1500 (200)	560	170	85	35	2.6	0.38	0.14		0.04 (0.008)
44K/0.7K	1500 (200)	510		70		2.0	0.26	0.08	0.04	0.02 (0.005)

[a] The viscosities for the pure melts at 110.5 °C are in parentheses.

melts and binary mixtures, were hermetically sealed under N_2 in 7 mm od NMR sample tubes and equilibrated for several weeks.

Pulsed-gradient NMR spin echo diffusion experiments in the proton resonance, as well as occasional transverse relaxation measurements, were carried out on a 33 MHz spin-lock CPS-2 spectrometer operating with a wide-gap electromagnet. Gradient coils in the Zupančič-Pirš configuration supplied horizontal gradients of calibrated magnitude of 573 G/cm at the measurement temperature of 110.5 °C. Principal echo transverse magnetization decays, where measured, were nonexponential but unimodal, with T_2 ranging between 15 and 120 ms.

The nonspectroscopic PG-NMR experiments were performed at fixed G by varying the duration δ of each of the pair of gradient pulses coordinated with the stimulated-echo radio-frequency (rf) pulse sequence. In this work the rf pulse spacing τ_1 between the first two 90° pulses was 18 ms, and the spacing between the first and third pulses, hence also the spacing Δ between the gradient pulses, was 100 ms for samples exhibiting faster diffusion and 200 ms for samples in which at least one of the components diffused slowly. To minimize residual gradient effects, δ was never larger than $\tau_1 - 6$ ms but usually did not exceed 3 ms. A steady gradient $G_0 = 0.35$ G/cm parallel to G was used for convenience in data collection. Between 8 and 12 values of δ were employed to produce a maximal echo attenuation to below 3% of the original echo. Signal averaging of between 5 and 20 passes for each δ improved the signal-to-noise ratio. Experiments were conducted off-resonance by −3 kHz in single-sideband mode with single-phase rf phase-sensitive detection, and the echo signal A was measured as the integral over the magnitude Fourier transform of the beat between echo and reference, after correction for rms baseline noise. Several independent checks revealed no explicit dependence of the extracted diffusion coefficient on Δ, ensuring that the diffusion was Fickian.

Data reduction was performed off-line by the current PC version of a FORTRAN program[50] which accounts for residual gradient effects,[51] known polymer polydispersity,[52] and multicomponent diffusion.[52,53] The measured echo attenuation curves in all of our melts reflected a modest, smooth D distribution. The expression fitted to the data had the general form

$$\frac{A(X)}{A(0)} = \sum_i^N w_i \exp\left(-\frac{2\tau_1}{T_{2i}}\right) \exp(-\gamma^2 D_i X) \qquad (1)$$

where $X = (G\delta)^2(\Delta - \delta/3)$ with small additional terms in GG_0; γ denotes the protons' gyromagnetic ratio. The normalized sum over $N = 10$ terms simulated a diffusivity distribution based on the known polydispersity ratio assuming a log−normal molecular weight distribution. This model[52] coordinates weights w_i with corresponding molecular weight fractions M_i and maps these onto diffusivities D_i, optimally adjusting D at the reference molecular weight, $D(M_n)$ in melts; in binary mixtures

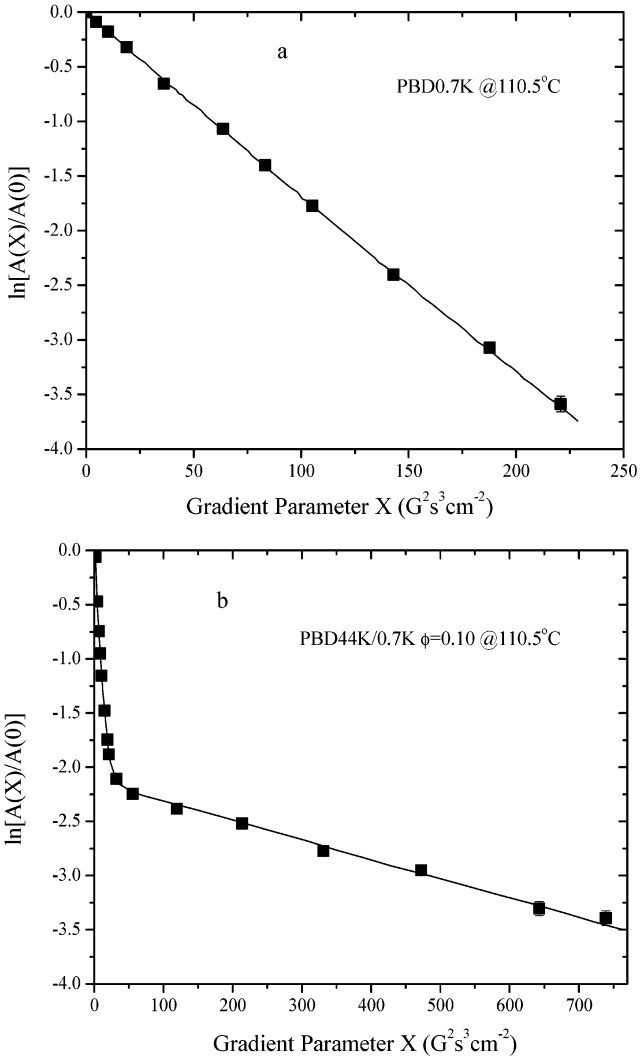

Figure 1. Typical PG-NMR attenuation of echo-signal intensity for the pure polymer (a) PBD0.7K and the mixture (b) of PBD44K/0.7K at $\phi = 10\%$ at 110.5 °C.

two components are accommodated, resulting in fitted parameters D_{fast} and D_{slow}. The estimated weak dependence of T_2 on molecular weight in the ensemble was also routinely included in the fitted model. The resulting fits were successful in all cases. Typical echo attenuation plots for both a pure melt and a blend including the fit are shown in Figure 1a,b. The diffusion coefficients obtained for both components in the binary mixtures in this way are listed in Table 3. All data in Table 3 carry an experimental error of at least 5%.

Table 3. Diffusivities of PBD Long Chains and Short Chains[a] in the Mixtures at 110.5 °C

	D_s (10^{-10} cm^2/s) at ϕ =									
mixture	1.0	0.8	0.6	0.5	0.4	0.2	0.1	0.05	0.02	0
44K/12K	2.6	3.2	3.7	4.1	4.5	7.4	18	18		
	(57)[b]	(63)	(60)	(63)	(63)	(72)	(83)	(83)		(72)
44K/8.9K	2.6	3.3		4.2		8.3	19	38		
	(91)	(100)		(110)		(130)	(140)	(160)		(150)
44K/5.8K	2.6	3.2		4.4		10	25	50		
	(240)	(280)		(310)		(360)	(410)	(460)		(450)
44K/3.9K	2.6	3.2	4.2	4.8	5.9	16	36	120		
	(610)	(620)	(690)	(720)	(780)	(930)	(1000)	(1200)		(1200)
44K/2.0K	2.6	3.4		5.6		20	47	72		
	(2300)	(2500)		(3200)		(3900)	(4200)	(4500)		(4500)
44K/1.0K	2.6	3.8	5.6	7.4	11	48	200	580		
	(4900)	(6200)	(7400)	(8200)	(9100)	(10000)	(13000)	(14000)		(15000)
44K/0.7K	2.6	3.8		8.1		60	260	620	3200	
	(7100)	(8900)		(12000)		(17000)	(20000)	(24000)	(24000)	(24000)
12K/0.7K	72	120		290		1100	2000			
	(7100)	(9100)		(13000)		(18000)	(20000)			(24000)
3.9K/0.7K	1200	1400		2600		4900	11000			
	(7100)	(8600)		(14000)		(19000)	(25000)			(24000)

[a] The diffusivities of PBD short chains in the mixtures are in parentheses. [b] The diffusivities of PBD short chains at $\phi = 1.0$ were obtained by extrapolation shown in Figure 8.

III. Theoretical Section

Our data analysis in the next section requires a brief overview of the theoretical ingredients in the description of the terminal dynamics of the long chain in a binary mixture in terms of its reptation in a dilated tube with an impeded curvilinear diffusivity D that depends on the short chain length N_S and on the weight fraction ϕ of the long chain in the mixture. The terminal relaxation time τ_d for the mixtures is related to that of the pure long chain melt, $\tau_{d0}^{CLF}(N_L)$, through the dilation tube length $L_{CLF}(\phi)$ and curvilinear diffusivity D as[11]

$$\tau_d(N_L,N_S,\phi) = L_{CLF}^2(\phi)/D(N_L,N_S,\phi) = \tau_{d0}^{CLF}(N_L)\, h(N_S,\phi) \tag{2}$$

where h is given by

$$h(N_S,\phi) = (a/a_L)^2\lambda(N_S,\phi)\frac{(1 - Xa_L/R_L)^2}{(1 - Xa/R_L)^2} \tag{3}$$

with $\lambda = D_c/D$ and $R_L = N_L b^2$, and all the other quantities already introduced and defined in ref 11. Note that the description of the contour length fluctuation in eq 3 is not expected to hold for when R_L/a_L is not large enough.

The zero-shear viscosity η of binary mixtures can be approximately related to the zero-shear viscosity η_0 of the long chain melt as

$$\eta(N_L,N_S,\phi) = \eta_0\left[\left(\frac{G_{pl}}{G_N^0}\right)h(N_S,\phi) + \left(1 - \frac{G_{pl}}{G_N^0}\right)\left(\frac{N_S}{N_L}\right)^3\frac{(1 - Xa/R_S)^2}{(1 - Xa/R_L)^2}\right] \tag{4}$$

with $\eta_0 = G_N^0\tau_{d0}^{CLF}(N_L)$ for the pure long chain melt according to Doi and Edwards,[2] where G_N^0 is the plateau modulus of the melt and G_{pl} is the terminal plateau modulus. The second term in eq 4 roughly accounts for the short chains' contribution: $(G_N^0 - G_{pl})\tau_{d0}^{CLF}(N_S) = \eta_0(1 - G_{pl}/G_N^0)[\tau_{d0}^{CLF}(N_S)/\tau_{d0}^{CLF}(N_L)]$. It can be shown[11,54] that the tube dilation factor (a_L/a) is related to G_{pl} as

$$G_{pl} = G_N^0\phi(a/a_L)^2 \tag{5}$$

The dependence of η on N_S arises from that of τ_d through the impedance function λ in eqs 2 and 3 and from the second term in eq 4.

When short chains are incorporated into the long chain melt, they dilate the confining tube, within which the long chain would reptate with an impeded curvilinear diffusivity $D = D_c/\lambda$. As long as the weight fraction of the long chain ϕ and/or the long chain length N_L is sufficiently high, the long chains would remain entangled with one other. Under this condition, the standard expression for the ideal self-diffusion coefficient of the *pure* long chain melt without any CR correction

$$D_{rep0}(N_L) = R_L^2/\tau_{d0} = (N_e/N_L)D_c \tag{6}$$

can be readily generalized to yield the self-diffusion coefficient D_{rep} for the long chain in the binary mixture

$$D_{rep}(N_L,N_S,\phi) = D_{rep0}(N_L)(a_L/a)^2/\lambda(N_S,\phi) \tag{7}$$

Equation 7 is derived from $D_{rep} = R_L^2/\tau_{rep}$, where

$$\tau_{rep}(N_L,N_S,\phi) = L^2(\phi)/D \tag{8}$$

or by analogy to replace in eq 6 D_c with $D = D_c/\lambda$ and N_e with

$$N_e(\phi) = N_e(a_L/a)^2 \tag{9}$$

to reflect the tube dilation. A recent survey of the available literature data showed[28] that for chain length N_L less than $20N_e$ there can be a significant deviation even in monodisperse melts from the ideal reptative diffusion due to mobile obstacles forming the tube, which is known as the CR effect. For binary mixtures and entangled solutions, the CR effect can be shown to be greater than in the pure melt since the CR correction is measured in terms of the tube diameter. Specifically, because of the CR effect, the chain gains an additional factor of

$$D_{CR} = \frac{R_L^2}{\tau_{rep}[N_L/N_e(\phi)]^2} \tag{10}$$

in its self-diffusion, where the denominator depicts the dynamics of Rouse-like (dilated) tube reorganization, with τ_{rep} given by eq 8. Building in this CR correction, we arrive at the following expression for the self-diffusion coefficient of the long chain in a binary mixture of short and long chains

$$D_s(N_L,N_S,\phi) = D_{rep} + AD_{CR} = D_{rep}(N_L,N_S,\phi)[1 + A(N_e/N_L)^2(a_L/a)^4] \quad (11)$$

where the prefactor A is between 10 and 20 and use has been made of eqs 7, 9, and 10. The tube dilation factor a_L/a has been experimentally found[11,40] to scale with ϕ as $\phi^{-0.6}$ because the terminal modulus in eq 5 has been found to scale like $\phi^{2.2}$. Although eq 11 contains the account of the CR effect in diffusion, it is not to be taken as quantitatively reliable.

IV. Results and Discussion

A. Rheological Measurements. The first set of experiments involved oscillatory shear measurements of binary mixtures made of the long chain with molecular weight equal to 44K in different short chains of molecular weights 12K, 8.9K, 5.8K, 3.9K, 2.0K, 1.0K, and 0.7K. The weight fraction of 44K in the binary mixtures varied from 0 to 1. We need first to establish the condition under which the crossover frequency ω_c can be identified as the terminal relaxation time of the long chain. The condition is that the shapes of G' and G'' in the terminal regime are invariant with respect to the weight fraction ϕ of the long chain and identical to those of the pure long chain melt. The preserved feature ensures that the short chain dynamics are sufficiently faster so as to result in negligible contributions to G' and G'' at frequencies at and below ω_c and that the long chain's dynamics remain reptative despite the tube dilation. So in our binary mixtures the short chains merely cause tube dilation and modify the curvilinear diffusivity D to make it dependent on both the short chain length N_S and a_L or ϕ. Thus, as long as the shape of the terminal region defined by G' and G'' is preserved, the crossover point ω_c, where $G'(\omega_c) = G''(\omega_c)$, can be identified as the terminal relaxation rate associated with the long chains, i.e., $\tau_d = 1/\omega_c$. To verify this point, master curves in the terminal region were shifted according to the position of the crossover point corresponding to that of the pure 44K melt. The shifted master curves for the 44K/1.0K system and the 44K/12K system are shown in Figure 2a,b.

Figure 2a shows that down to $\phi = 0.2$ the shapes of G' and G'' remain identical to those of the pure 44K melt for the mixtures involving the short chain of 1.0K. It means that at $\phi = 0.2$ the solution is still well entangled. For short chains of higher molecular weights, a significant contribution comes from the short chains in the terminal region, especially at low values of ϕ. Figure 2b indicates that the terminal shapes of the G' and G'' spectra cannot be preserved beyond $\phi = 0.5$ for the mixtures of 44K/12K.

Because of the much more rapid disentanglement of the short chains, only long chains can provide tube confinement for one another at long times.[11,55] Consequently, the long chains find themselves restricted to reptate a dilated tube. The dimension of the dilated tube can be shown[54] to be related to the terminal plateau modulus G_{pl} as $G_{pl} = G_N^0\phi(a/a_L)^2$, where a and a_L are the diameters of the bare and dilated tubes, respectively.

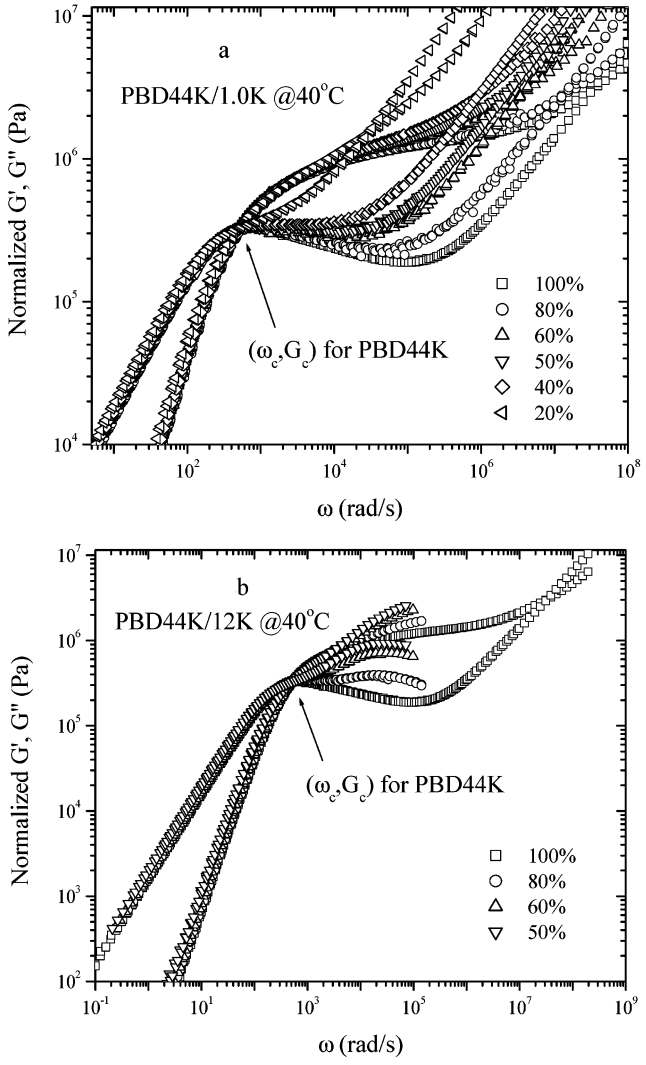

Figure 2. Two normalized master curves for PBD44K in the short chains (a) PBD1.0K and (b) PBD12K, all shifted to the crossover point of the pure PBD44K, where both the crossover frequency ω_c and modulus G_c are indicated.

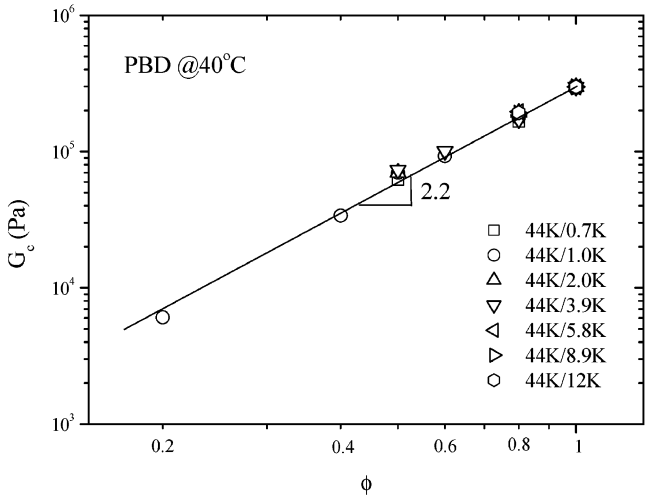

Figure 3. Crossover modulus G_c for PBD mixtures at 40 °C.

Since $G_c = G'(\omega_c) = G''(\omega)$ is proportional to G_{pl},[11] Figure 3 on the ϕ scaling of G_c confirms through eq 5 the previously reported ϕ dependence[11,40] of $a_L \propto \phi^{-0.6}$.

All the zero-shear viscosities for the pure melts and binary mixtures are listed in Table 2 and also shown in

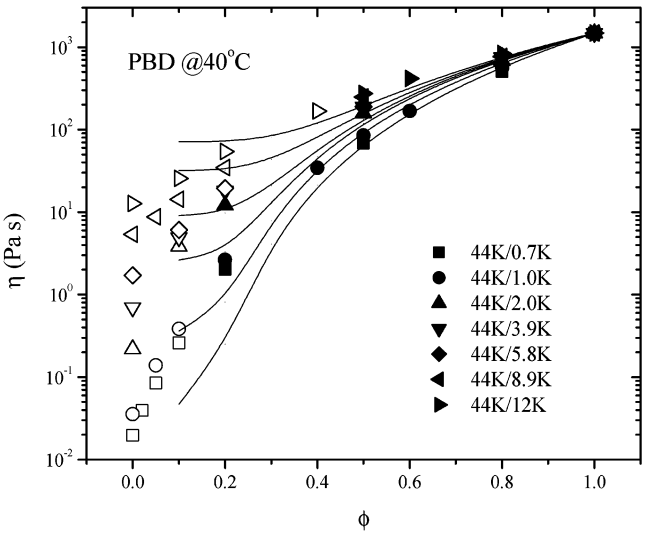

Figure 4. Zero-shear viscosities η for PBD mixtures at 40 °C, where the symbols are experimental data and the lines are theoretical predictions. The open symbols represent mixtures that are either hardly entangled or the short chains make a significant contribution to the overall viscosity.

Figure 4. Similar to the results for PBD binary systems in the previous publications,[11,40] the effect of short chains on the concentration dependence of the zero-shear viscosity η_0 is rather significant. When the short chain is unentangled, i.e., which is the case for $M = 0.7$K and 1.0K, the second term in eq 4 is negligible, and we would get a scaling exponent of 3.4 for the ϕ dependence to arise from the tube dilation alone according to eq 4. An additional free volume correction make the exponent larger than 3.4, similar to previous findings for concentrated polymer solutions.[56] When the short chain is relatively long such as in the mixture of 44K and 12K, the zero-shear viscosity contains an appreciable contribution from the short chain component, especially at low ϕ, and eq 4 does not hold well. The solid curves in Figure 4 are the theoretical predictions for various binary mixtures according to eq 4, where the λ parameter is treated as an input parameter from the subsequent Figure 5c. The solid symbols are the viscosity data for the systems having the meaningful crossover point in the master curves, while the open symbols are for the rest. The same notation is applied in the following figures and text unless specified otherwise. The prediction appears reasonably good for the solid symbols. For the 44K/12K mixtures, the deviation between the experimental data and the prediction based on eq 4 becomes large as expected.

From the oscillatory shear measurements, we also obtain the terminal relaxation times τ_d associated with the linear chains in the binary mixtures as a function of composition and short chain length by equating τ_d with the reciprocal of the crossover frequency ω_c, which has been identified in Figure 2a,b. Figure 5a shows that τ_d is dependent on the short chain length N_S at all concentrations. This systematic variation with N_S can be accounted for by recognizing that the impedance parameter λ defined eqs 2 and 3 is an explicit function of N_S. Such behavior has been observed in our previous rheological study[11] of binary mixtures where the long chains were much longer.

In our previous work, an enhanced contour length fluctuation (CLF) effect[11] was found in PBD binary mixtures associated with the terminal relaxation dy-

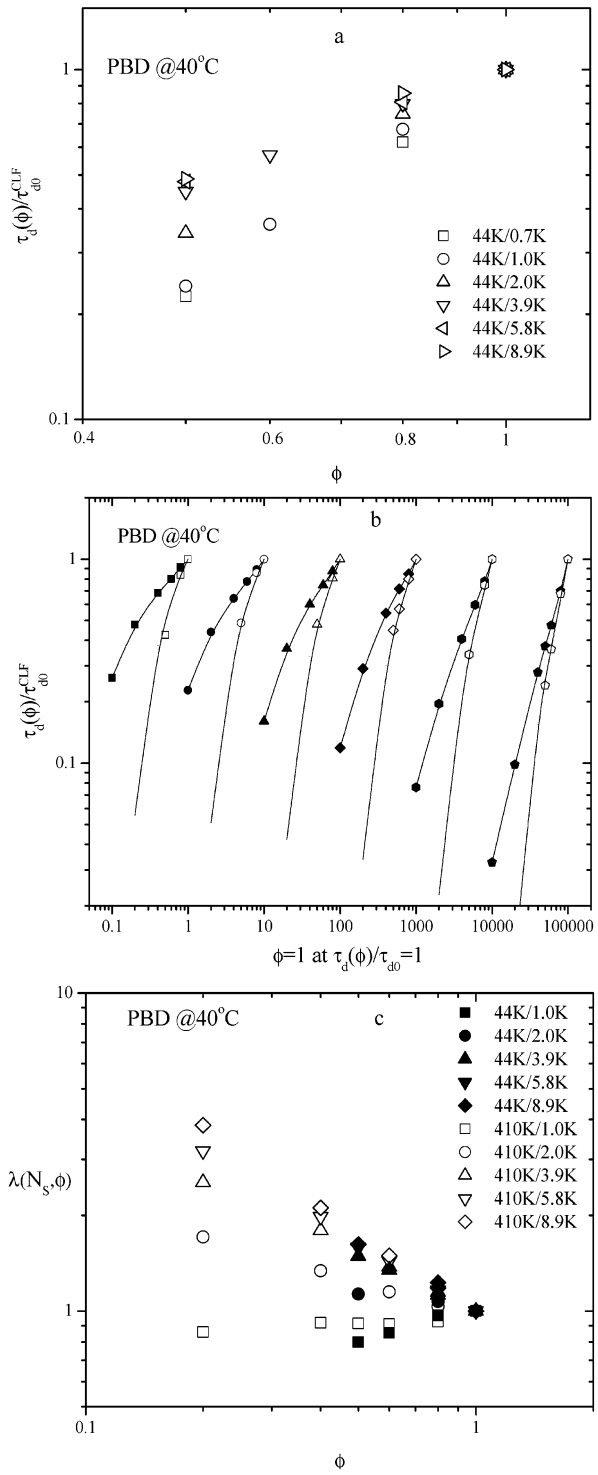

Figure 5. (a) The normalized terminal relaxation time as a function of concentration in binary mixtures of 44K with different short chains. (b) The normalized terminal relaxation time as a function of concentration in binary mixtures involving long chains of two different molecular weights $M_w = 410$K (solid symbols) and 44K (open symbols) in the same short chains of 12K (squares), 8.9K (circles), 5.8K (triangles), 3.9K (diamonds), 2.0K (hexagons), and 1.0K (pentagons). The curves show the theoretical prediction of the enhanced contour length fluctuation effect for the two different long chain lengths at various concentrations. On the *x*-axis, every decade represents the same range of concentration from 0.1 to 1 so that all the data and predictions can be presented in a single figure. (c) Impedance function λ for the 44K mixtures (solid symbols) evaluated from eqs 2 and 3 after inserting the relaxation time's concentration dependence in (b) and $(a_L/a)^2 \propto \phi^{-1.2}$ and for the 410K mixtures (open symbols) obtained previously.

namics of the long chains. As indicated in eq 3, the CLF factor is more significant for a larger a_L or lower value of ϕ as well as for a smaller chain size R_L. We illustrate in Figure 5b the greater CLF effect on the mixtures involving 44K than that on the mixtures involving 410K, where the relaxation times for 410K and 44K in mixtures with different short chains are estimated from the crossover frequencies in the master curves after examining the validity of the terminal region as described above. For the same short chains the normalized terminal relaxation times are experimentally found to decrease more strongly with lowering ϕ for the 44K mixture. In other words, the splits between the open and filled symbols are due mostly to the difference of the CLF effect between the two sets of mixtures. This is also anticipated theoretically by eq 3: At any concentrations, the difference in the normalized relaxation times corresponding to 410K and 44K long chains can be written in terms of the ratio of the normalized time for 410K to that for 44K

$$\frac{(\tau_d/\tau_{d0}^{CLF})_{44K}}{(\tau_d/\tau_{d0}^{CLF})_{410K}} = \frac{[1 - X(a_L/R_{44K})]^2[1 - X(a/R_{410K})]^2}{[1 - X(a_L/R_{410K})]^2[1 - X(a/R_{44K})]^2} \quad (12)$$

where R_{410K} and R_{44K} are the mean chain end-to-end distances for the chains of molecular weights 410K and 44K, respectively. On the basis of the experimental data for the 410K mixtures, we can predict how the normalized relaxation times of 44K mixtures would vary for different ϕ and N_S as shown in Figure 5b. The split between 410K and 44K systems is independent of the short chain length and is more severe at low concentrations. This conclusion is consistent with our previous results[11] for binary mixtures involving the PBD long chains of 410K, 207K, and 100K with a fixed short chain of 12K.

Figure 3 indicates through eq 5 that the tube dilation factor in eq 3 scales as $(a_L/a)^2 \propto \phi^{-1.2}$. Substituting this experimental result and the data in Figure 5a or 5b into eq 2 via eq 3, we reveal as done previously[11] how the parameter λ varies with the short chain length at different concentrations. Figure 5c shows this extracted function for these mixtures and compares it with that obtained previously[11] for mixtures involving 410K long chain. The two sets of data indicate a similar trend as expected.

B. Diffusion Measurements. *1. Long Chain's Self-Diffusion in Binary Mixtures with Different Short Chains.* To complement the systematic rheological data, we have carried out self-diffusion measurements of the same binary mixtures using the PG-NMR method as described in section II. Figure 6 shows the self-diffusion coefficient of 44K as a function of concentration in its different binary mixtures. The numerical values have also been provided in Table 3. All the diffusion measurements are performed at 110.5 °C. Similar to Figure 5a for the terminal relaxation time, the self-diffusion coefficient D_s also displays a systematic variation with the molecular weigh N_S of the second component due to the same physical origin: The curvilinear diffusivity D in eq 2 or the impedance parameter $\lambda = D_c/D$ in eq 7 depends explicitly on N_S. There is no other known physical process that would produce this N_S dependence. A theoretical prediction using eq 11 is also shown in Figure 6. The theoretical account given in eq 11 appears to describe the data very well. It is necessary to mention that eq 11 requires the value of λ in eq 7 as the input

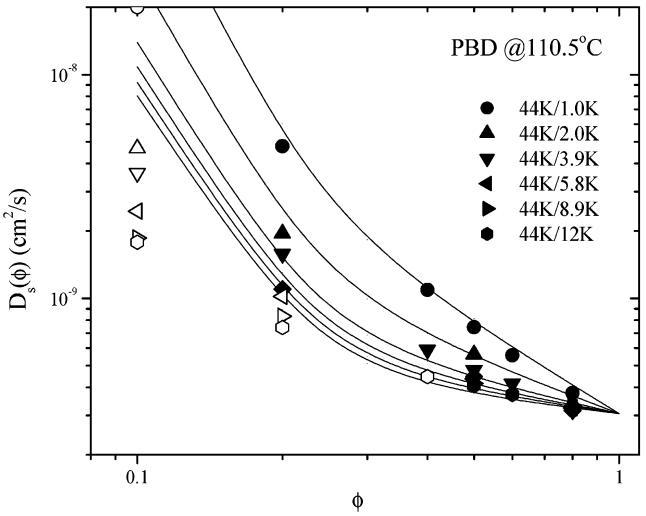

Figure 6. Self-diffusion coefficient D_s for PBD44K in its mixtures at 110.5 °C, where the symbols are experimental data and the lines are theoretical predictions and the open symbols carry the same meaning as in Figure 4.

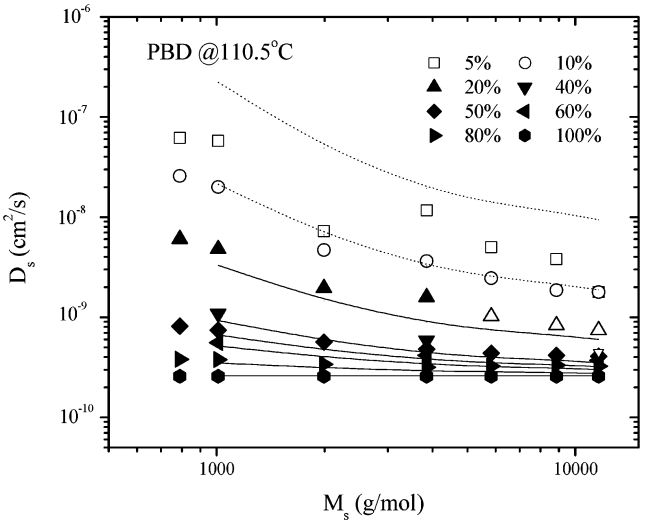

Figure 7. Matrix molecular weight dependence of self-diffusion coefficient D_s of PBD44K in different short chain matrices at 110.5 °C, where the symbols are experimental data and the lines are theoretical predictions.

parameter, which can be obtained as shown in Figure 5c from the rheological data given in Figure 5a. In other words, the theoretical curves are made by inserting the values for the λ parameter from Figure 5c into eq 11.

The diffusion coefficient D_s increases monotonically with decreasing ϕ until the diffusion measurement can no longer select out the signal due to the long chain's self-diffusion at very low ϕ, which is about 5% for 44K here. Complementary to the data for the terminal relaxation time in Figure 5a, D_s of the long chain in the binary mixtures shows not only composition dependence but also dependence on the short chain length N_S, and the concentration dependence is stronger for shorter chain lengths. The open symbols are for systems barely entangled or systems where there is no longer a clear separation between the dynamics of long and short chains, for which the theoretical description of eq 11 does not apply. Figure 6 can also be represented in terms of the short chain length at different concentrations as shown in Figure 7. The theoretical description of eq 11 based on the concept of tube dilation and

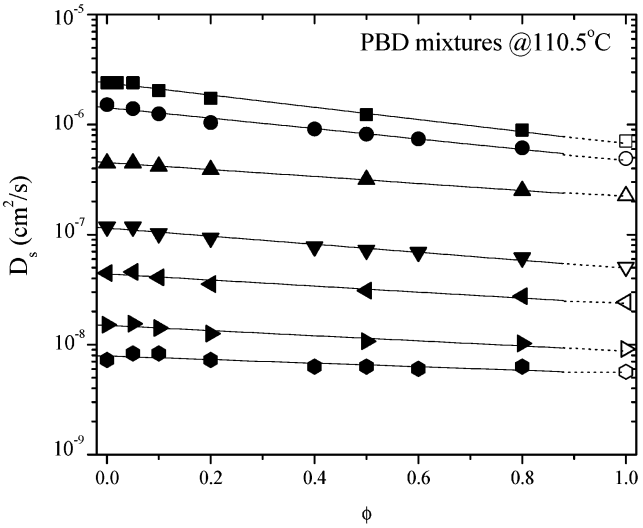

Figure 8. Self-diffusion coefficient D_s for PBD short chains in their mixtures with 44K at 110.5 °C from top to bottom: 44K/0.7K, 44K/1.0K, 44K/2.0K, 44K/3.9K, 44K/5.8K, 44K/8.9K, 44K/12K.

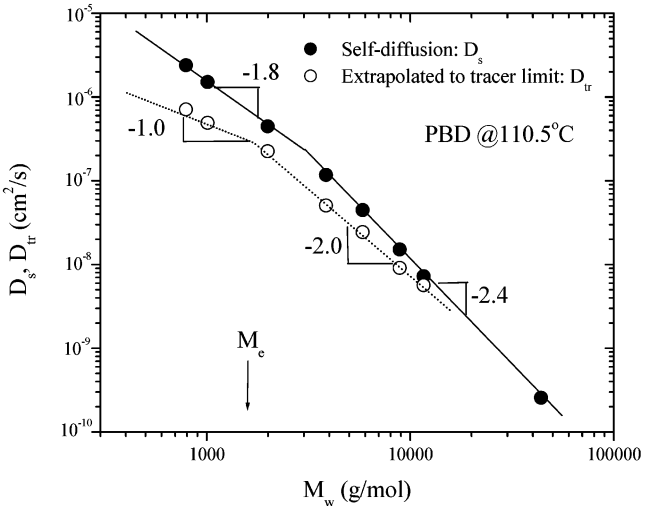

Figure 9. Molecular weight dependence of diffusion coefficients of PBD samples at 110.5 °C, where solid circles denote the self-diffusion coefficient and open circles are the values extrapolated to the trace limit from Figure 8.

impeded curvilinear diffusion is remarkably good up to 10%. More importantly, Figures 6 and 7 provide independent experimental evidence that the long chain dynamics vary systematically with the short chain length and is accelerated by the presence of short chains even when the short chains are relatively long such as in the mixture of 44K and 12K. These observations, although accountable in our current theoretical framework as described in section III and previously,[11] are in contradiction with the previous theories of Doi et al.[34] that would predict D_s to be independent of N_s and of Viovy et al.[35] that would predict D_s to be independent of ϕ for the 44K/12K mixtures.

2. Short Chain's Self-Diffusion in Binary Mixtures with a Long Chain. As explained in section II, the PG-NMR spin echo measurements allow us to evaluate self-diffusion coefficients in binary mixtures for both long and short chains. Thus, besides the measured self-diffusion coefficient D_s shown in Figure 6 for the long chain of 44K in its mixtures, we can also determine D_s associated with the short chains at different weight fractions of the 44K long chains. The results are listed in Table 3 and plotted in Figure 8. The first thing to note in Figure 8 is that D_s of the short chain is higher in the absence of 44K long chains, i.e., at $\phi = 0$, and decreases systematically with increasing weight fraction ϕ of the long chains. We may actually extrapolate this trend all the way to the trace limit (i.e., $\phi = 1$) of few short chains diffusing in the matrix of 44K, which is represented by the open symbols in Figure 8. In this limit, the constraint release (CR) effect on the short chain diffusion is minimized. The second thing to note is that the increase of D_s with lowering ϕ is stronger for shorter chains, implying the CR effect is larger for smaller N_S as expected. The variation for the lowest N_S with ϕ has another source: the lower glass transition temperatures or higher free volumes.

An important byproduct of Figure 8 is the extrapolated values for D_s of the short chains in the matrix of 44K as denoted by the open symbols. These values can be approximately taken as the trace diffusion coefficient D_{tr} for these chains of different lengths. The difference between D_{tr} at $\phi = 1$ and D_s measured in itself (i.e., $\phi = 0$) is evident from Figure 8 and can be more explicitly illustrated in Figure 9. The data in Figure 9 support the idea[28] that the nonreptative scaling of D_s with molecular weight arises from the appreciable constraint release effect, which can be diminished as represented by the trace diffusion coefficient in the open symbols. In other words, the asymptotic reptative scaling with exponent 2.0 can be approximately recovered by more permanent tube confinement. Moreover, the deviation from the reptative scaling does not appear to originate from the contour length fluctuation (CLF) effect as previously speculated[57] because the trace diffusion would also suffer from the CLF effect and would not display the pure reptative scaling.[28] To our knowledge, this is the first time when the data from PG-NMR measurements have been extrapolated to extract a trace diffusion coefficient in polymer blends.

The much stronger molecular weight dependence of D_s in the Rouse regime has been observed before,[20] where the free volume effect is rather severe.[58] By extrapolating to the trace diffusion limit as done in Figure 9, we are able to recover the condition of common monomeric friction coefficient and restore the expected molecular weight scaling for the ideal Rouse diffusion coefficient.

To further illustrate the free volume correction to the monomeric friction coefficient involved in both viscosity and diffusion coefficients, we present the molecular weight dependence of the zero-shear viscosity at both 40 and 110.5 °C shown in Figure 10a. The data of Colby et al.[58] and Watanabe et al.[59] are also included to show that our data match exactly with their data, where the data at 110.5 °C were obtained from the raw data reported in ref 58 using the WLF relation. The open and solid symbols are the raw data before and after isofriction correction, respectively. It can be shown[58] that the data for oligomeric PBD at any finite temperature can be lifted upward by a factor of $\exp[2.303(c_{1\infty} - c_1)]$ to eliminate the free volume effect, where $c_{1\infty}$ and c_1 are the WLF factors at the reference temperature T for a sufficiently high molecular weight PBD and the oligomeric PBD, respectively. Since our raw data overlap with the raw data as shown by the open symbols in Figure 10a, we can expect the same isofriction correction for our samples. The viscosity of 1,4-PBD at higher

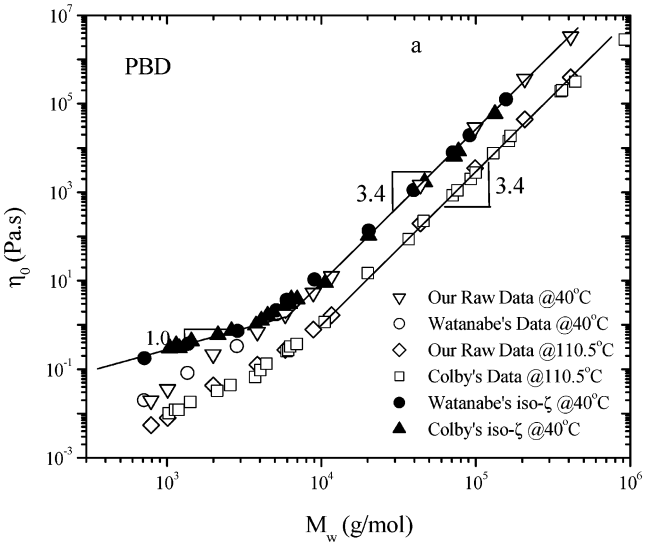

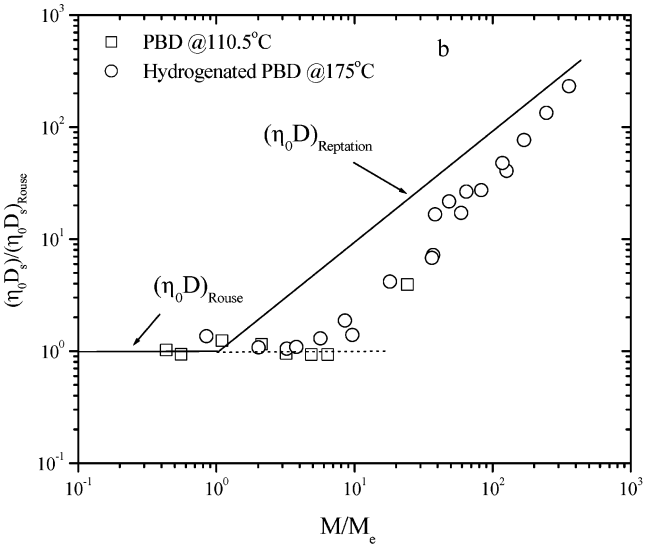

Figure 10. (a) Molecular weight dependence of zero-shear viscosity η_0 for 1,4-polybutadiene at 40 and 110.5 °C, along with literature data from refs 58 and 59 with and without isofriction correction. (b) Product of $\eta_0 D$ normalized by $(\eta_0 D)_{\text{Rouse}}$ as a function of M/M_e for 1,4-polybutadiene at 110.5 °C and hydrogenated polybutadiene at 175 °C from ref 21.

molecular weights from our previous study[11] is also plotted along with the current measurements at molecular weights up to 44K. The viscosity at 110.5 °C is obtained from that at 40 °C by using the WLF relation previously obtained.[11] It is evident that η_0 agrees very well with the literature at the two temperatures, showing the well-known $M^{3.4}$ scaling as expected in the entangled regime. In the Rouse regime, the molecular weight dependence of the viscosity at 40 °C is much stronger ($M^{2.0}$) than the linear dependence. The molecular weight dependence becomes weaker ($M^{1.8}$) at 110.5 °C and recovers the Rouse scaling after the isofriction correction.

Pearson et al.[21] first combined the viscosity and diffusion coefficient to cancel out the friction factor and temperature dependence. They also suggested that the product $\eta_0 D_s$ for pure melt and concentrated solutions of linear flexible polymers, normalized by the product in the Rouse regime, is a universal function of the number of chain entanglement. Assuming that D_s is related to the terminal relaxation time τ_d through the

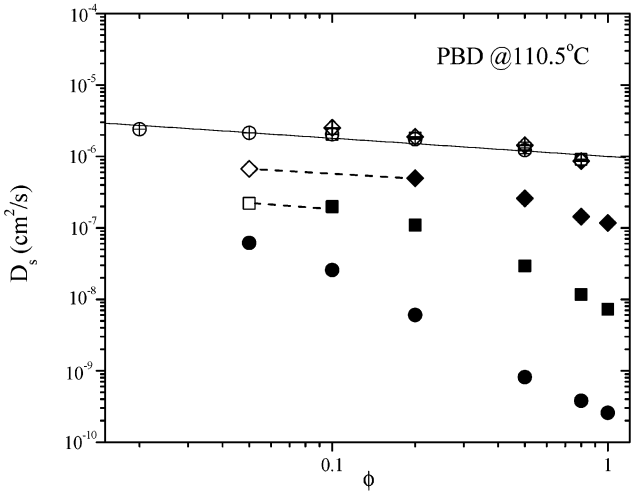

Figure 11. Self-diffusion coefficient D_s for PBD long chains of 44K (circles), 12K (squares), and 3.9K (diamonds) in a matrix of PBD0.7K and D_s for PBD0.7K in the same mixtures with 44K (open crossed circles), 12K (crossed squares), and 3.9K (crossed diamonds) at 110.5 °C. The open diamond and square are the extrapolated self-diffusion coefficients for the long chains to $\phi = 0.05$.

mean chain end-to-end distance R as $D_s = R^2/6\tau_d$, and η_0 is related to τ_d through the modulus G as $\eta_0 = G\tau_d$, one would show that $(\eta_0 D)_{\text{rep}}/(\eta_0 D)_{\text{Rouse}} = G_N^0/G_0 = M/M_e$, where G_0 and G_N^0 are the moduli in the Rouse and reptative regimes, respectively. Figure 10b displays the normalized $\eta_0 D$ at 110.5 °C for PBD together with the data for hydrogenated PBD at 175 °C in Pearson et al.'s work (see Figure 3b in ref 21). The experimental data fall considerably off from the theoretical anticipation represented by the line of slope 1, which is based on the assumption of the equivalence between chain relaxation and diffusion processes. This disagreement between experiment and theory has been suggested[28] to indicate that the scaling relation $D_s = R^2/6\tau_d$ cannot be valid except in the asymptotic limit of pure reptation at sufficiently high values of M/M_e.

3. Diffusion in Binary Mixtures of Entangled and Unentangled Chains. We have also carried out PG-NMR measurements of long chain solutions where the solvent is the oligomeric PBD of 0.7K. At various concentrations, the self-diffusion coefficients of both long chains of 44K, 12K, and 3.9K and the short chain of 0.7K can be determined as shown in Figure 11. Several key results are as follows. The self-diffusion coefficient D_s for the 0.7K Rouse melt is independent of the long chain's molecular weight, as one would expect from the Rouse model. The observed concentration dependence arises from the free volume effect as indicated in the previous subsection. At lowest concentrations of $\phi = 0.2$ for 3.9K, 0.1 for 12K, and 0.05 for 44K, respectively, the long chains are no longer entangled with one another in the respective three mixtures. We may extrapolate the values for D_s all the way to the concentration of 0.05 as shown by the two dashed lines in Figure 11 to properly account for the free volume effect. Reading from the extrapolated values of D_s at $\phi = 0.05$, we find that D_s is inversely proportional to M as shown in Figure 12, indicating Rouse-like dynamics for the embedded long chains in the short chain of 0.7K. In other words, the 0.7K short chains appear to be able to screen the hydrodynamic interactions. At sufficiently high values of ϕ, the long chains are entangled with each other and their self-diffusion coefficient D_s drops sharply. The

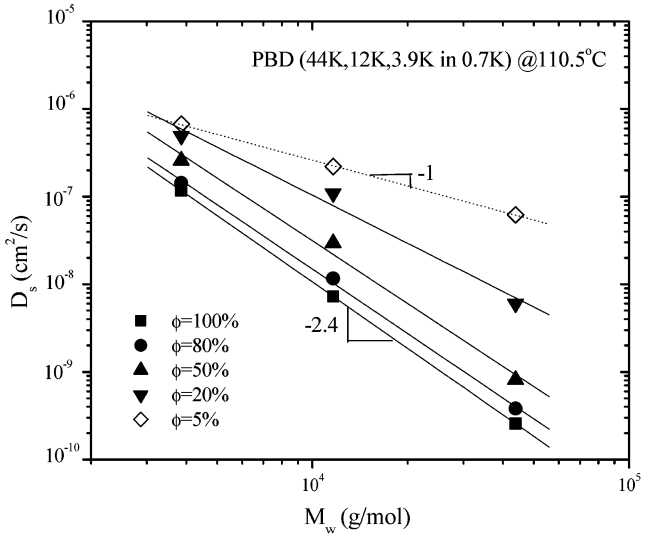

Figure 12. Molecular weight dependence of self-diffusion coefficient D_s of different PBD long chains in PBD0.7K at different concentrations at 110.5 °C.

trend from Rouse-like dynamics to reptation like dynamics can be more explicitly illustrated by plotting D_s as a function of the long chain's molecular weight at the different concentrations as shown in Figure 12. We see that the scaling law smoothly switches from the Rouse-like M^{-1} to the reptation-like $M^{-2.4}$ as the weight fraction of the long chain in the binary mixtures increases from 5% to 100%.

V. Conclusion

In summary, we have carried out both rheological and diffusion measurements of 1,4-polybutadiene binary mixtures of long and short chains over the full composition range as a function of both long and short chain lengths. The rheological characterization of these binary mixtures is consistent with our previous results.[11] The independent diffusion measurements confirm the rheological observations that the terminal relaxation time τ_d due to the long chains in the mixtures increases with the short chain length N_S and with the weight fraction ϕ of the long chains. In other words, the measured self-diffusion coefficient D_s of the long chain is found to be systematically larger for a shorter N_S at any given composition. The notions[11] of tube dilation and impeded curvilinear diffusivity can be applied to depict the experiment. Since the PG-NMR spin echo technique allows determination of the self-diffusion coefficients of both long and short chains in a binary mixture, we are also able to obtain not only the diffusion coefficient $D_s(N_S,\phi)$ of the short chain as a function of N_S at various values of ϕ but also the trace diffusion coefficient D_{tr}, i.e., $D_s(N_S,\phi)$ in the limit of $\phi = 1$, which corresponds to embedding the trace short chain in a matrix of long chains. In agreement with other data in the literature as reviewed recently,[28] it is found that D_{tr} shows a reptative scaling of $D_{tr} \propto M^{-2.0}$ whereas D_s scales nonasymptotically as $D_s \propto M^{-2.4}$. The PG-NMR method has also been applied to reveal that the short chain's self-diffusion coefficient in its binary mixtures with other long chains remains the same independent of the long chain length at any given composition. This result although expected clearly demonstrates the concept of critical molecular weight M_e for entanglement and the presence of a mesh size defined by M_e.

Acknowledgment. This work was supported, in part, by NSF Grant DMR 01-96033 and the Ohio Board of Regents.

References and Notes

(1) de Gennes, P. G. *J. Chem. Phys.* **1971**, *55*, 572. de Gennes, P. G. *Scaling Concepts in Polymer Physics*; Cornell University Press: Ithaca, NY, 1979.
(2) Doi, M.; Edwards, S. F. *The Theory of Polymer Dynamics*, 2nd ed.; Clarendon Press: Oxford, England, 1988.
(3) Rubinstein, M. *Phys. Rev. Lett.* **1987**, *59*, 1946. Rubinstein, M. In *Theoretical Challenges in the Dynamics of Complex Fluids*; McLeish, T. C. B., Ed.; Kluwer Academic Publisher: Dordrecht, 1997.
(4) Tirrell, M. *Rubber Chem. Technol.* **1984**, *57*, 522.
(5) Bachus, R.; Kimmich, R. *Polymer* **1983**, *24*, 964.
(6) Klein, J. *Nature (London)* **1978**, *271*, 143. Klein, J.; Fletcher, D.; Fetters, L. J. *Nature (London)* **1983**, *304*, 526.
(7) Green, P. F.; Kramer, E. J. *Macromolecules* **1986**, *19*, 1108. Green, P. F.; Mills, P. J.; Palmstrom, C. J.; Mayer, J. W.; Kramer, E. J. *Phys. Rev. Lett.* **1984**, *53*, 2145.
(8) Watanabe, H.; Kotaka, T. *Macromolecules* **1984**, *17*, 2316.
(9) Ylitalo, C. M.; Kornfield, J. A.; Fuller, G. G.; Pearson, D. S. *Macromolecules* **1991**, *24*, 749.
(10) Juliani; Archer, L. A. *J. Rheol.* **2001**, *45*, 691.
(11) Wang, S.; Wang, S. Q.; Halasa, A.; Hsu, W. L. *Macromolecules* **2003**, *36*, 5355.
(12) Kim, H.; Chang, T.; Yohanan, J. M.; Wang, L.; Yu, H. *Macromolecules* **1986**, *19*, 2737.
(13) Wheeler, L. M.; Lodge, T. P. *Macromolecules* **1989**, *22*, 3399.
(14) Nemoto, N.; Kojima, T.; Inoue, T.; Hirayama, T.; Kurata, M. *Macromolecules* **1989**, *22*, 3793. Nemoto, N.; Kishine, M.; Inoue, T.; Osaki, K. *Macromolecules* **1991**, *24*, 1648.
(15) Komlosh, M. E.; Callaghan, P. T. *J. Chem. Phys.* **1998**, *109*, 10053.
(16) Tao, H.; Lodge, T. P.; von Meerwall, E. D. *Macromolecules* **2000**, *33*, 1747.
(17) Fleischer, G.; Appel, M. *Macromolecules* **1995**, *28*, 7281.
(18) Pearson, D. S.; Ver Strate, G.; von Meerwall, E.; Schilling, F. C. *Macromolecules* **1987**, *20*, 1133.
(19) Fleischer, G. *Colloid Polym. Sci.* **1987**, *165*, 89.
(20) Appel, M.; Fleischer, G. *Macromolecules* **1993**, *26*, 5520.
(21) Pearson, D. S.; Fetters, L. J.; Graessley, W. W.; Strate, G. V.; von Meerwall, E. *Macromolecules* **1994**, *27*, 711.
(22) Bartels, C. R.; Crist, B.; Graessley, W. W. *Macromolecules* **1984**, *17*, 2702.
(23) Gell, C. B.; Graessley, W. W.; Fetters, L. J. *J. Polym. Sci., Polym. Phys. Ed.* **1997**, *35*, 1933.
(24) Watanabe, H. *Prog. Polym. Sci.* **1999**, *24*, 1253.
(25) McLeish, T. C. M. *Adv. Phys.* **2002**, *51*, 1379.
(26) Doi, M. *J. Polym. Sci., Polym. Phys. Ed.* **1983**, *21*, 667.
(27) Milner, S. T.; McLeish, T. C. B. *Phys. Rev. Lett.* **1998**, *81*, 725.
(28) Wang, S. Q. *J. Polym. Sci., Polym. Phys. Ed.* **2003**, *41*, 1589.
(29) Graessley, W. W. *Adv. Polym. Sci.* **1982**, *47*, 68.
(30) Kotaka, T.; Adachi, K. *Macromol. Symp.* **1996**, *123*−*130*, 123.
(31) Adachi, K.; Itoh, S.; Nishi, I.; Kotaka, T. *Macromolecules* **1990**, *23*, 2554. Adachi, K.; Wada, T.; Kawamoto, T.; Kotaka, T. *Macromolecules* **1995**, *28*, 3588.
(32) O'Connor, N. P. T.; Ball, R. C. *Macromolecules* **1992**, *25*, 5677.
(33) Schweizer, K. S.; Fuchs, M.; Szamel, G.; Guenza, M.; Tang, H. *Macromol. Theory Simul.* **1997**, *6*, 1037.
(34) Doi, M.; Graessley, W. W.; Helfand, E.; Pearson, D. S. *Macromolecules* **1987**, *20*, 1900.
(35) Viovy, J. L.; Rubinstein, M.; Colby, R. H. *Macromolecules* **1991**, *24*, 3587.
(36) Masuda, T.; Kitagawa, K.; Inoue, T.; Onogi, S. *Macromolecules* **1970**, *3*, 116.
(37) Prest, W. M.; Porter, R. S. *Polym. J.* **1973**, *4*, 154.
(38) Montfort, J. P.; Marin, G.; Arman, J.; Monge, P. *Polymer* **1978**, *19*, 277.
(39) Montfort, J. P.; Marin, G.; Monge, P. *Macromolecules* **1984**, *17*, 1551.
(40) Struglinksi, M. J.; Graessley, W. W. *Macromolecules* **1985**, *18*, 2630.
(41) Kubo, T.; Nose, T. *Polym. J.* **1992**, *12*, 1351.
(42) Aslanyan, I. Yu.; Skirda, V. D.; Zaripov, A. M. *Polym. Adv. Technol.* **1999**, *10*, 157.
(43) von Meerwall, E.; Feick, E. J.; Ozisik, R.; Mattice, W. L. *J. Chem. Phys.* **1999**, *111*, 750.

(44) Rathgeber, S.; Wilner, L.; Richter, D.; Brulet, A.; Farago, B.; Appel, M.; Fleischer, G. *J. Chem. Phys.* **1999**, *110*, 10171.
(45) Smith, B. A.; Mumby, S. J.; Samulski, E. T.; Yu, L. P. *Macromolecules* **1986**, *19*, 470.
(46) Green, P. F. *J. Non-Cryst. Solids* **1994**, *172*−*174*, 815. Here the tracer chain is d-PS of 255 K in binary mixtures of 100K and 1800K PS. Thus, the tracer diffusion measurements do not yield any explicit information about the self-diffusion coefficients of the two components in the mixtures.
(47) Tead, S. F.; Kramer, E. J. *Macromolecules* **1988**, *21*, 1513.
(48) von Meerwall, E.; Wang, S.; Wang, S. Q. *Bull. Am. Phys. Soc.* **2002**, *47*, 1048. von Meerwall, E.; Wang, S.; Wang, S. Q. *Polym. Prepr.* **2003**, *44*, 287.
(49) Colby, R. H.; Milliman, G. E.; Graessley, W. W. *Macromolecules* **1986**, *19*, 1261.
(50) von Meerwall, E. D.; Ferguson, R. D. *Comput. Phys. Commun.* **1981**, *21*, 421.
(51) von Meerwall, E.; Kamat, M. *J. Magn. Reson.* **1989**, *83*, 309.
(52) von Meerwall, E.; Palunas, P. *J. Polym. Sci., Polym. Phys. Ed.* **1987**, *25*, 1439.
(53) Shim, S. E.; Parr, J. C.; von Meerwall, E. D.; Isayev, A. I. *J. Phys. Chem. B* **2002**, *106*, 12072.
(54) Graessley, W. W.; Edward, S. F. *Polymer* **1981**, *22*, 1329.
(55) Marrucci, G. *J. Polym. Sci., Polym. Phys. Ed.* **1985**, *23*, 159.
(56) Pearson, D. S. *Rubber Chem. Technol.* **1987**, *60*, 439.
(57) Frischknecht, A. L.; Milner, S. T. *Macromolecules* **2000**, *33*, 5273.
(58) Colby, R. H.; Fetters, L. J.; Graessley, W. W. *Macromolecules* **1987**, *20*, 2226.
(59) Watanabe, H.; Urakawa, O.; Yamada, H.; Yao, M.-L. *Macromolecules* **1996**, *29*, 755.

MA034835G